hydrology

MDPI

Article

Trends in Surface Water Quality and Trophic State in the Yucatán Peninsula over the Last Decade

Plutarco Hernández-Hernández [1], Laura Macario-González [2,*], Noel O. Cohuo-Zaragoza [1], Sergio Cohuo [1], Juan R. Beltrán-Castro [3], Lucía Montes-Ortiz [4], Leopoldo Q. Cutz-Pool [1] and Christian M. Huix [1]

1 Tecnológico Nacional de México/IT Chetumal, Av. Insurgentes 330, Chetumal, Quintana Roo 77013, Mexico; d12390410@chetumal.tecnm.mx (P.H.-H.); m20390653@chetumal.tecnm.mx (N.O.C.-Z.); sergio.cd@chetumal.tecnm.mx (S.C.); leopoldo.cp@chetumal.tecnm.mx (L.Q.C.-P.); d12390746@chetumal.tecnm.mx (C.M.H.)
2 Tecnológico Nacional de México/IT de la Zona Maya, Carretera Chetumal-Escárcega km 21.5, Quintana Roo 77965, Mexico
3 Centro de Bachillerato Tecnológico Industrial y de Servicios No. 253, Calle Sac-Xan 555, Col. Solidaridad, Chetumal, Quintana Roo 77086, Mexico; juan.beltran@cbtis62.edu.mx
4 Plantel San Felipe del Progreso, Universidad Intercultural del Estado de México, Libramiento Francisco Villa s/n, Col. Centro, San Felipe del Progreso 50640, Mexico; lucia.montes@uiem.edu.mx
* Correspondence: laura.mg@zonamaya.tecnm.mx

Abstract

Urbanization, expanding tourism, and infrastructure development are altering water quality in the Yucatán Peninsula (YP). This study evaluated temporal variations in water quality and trophic status using the Water Quality Index (WQI) and Trophic State Index (TSI) across ten inland water systems (IWS) monitored from 2012 to 2024. Spatial patterns from an additional 29 IWS sampled in 2024 were also analyzed. The Mann–Kendall test and Theil–Sen estimator revealed a significant decline in water quality ($Z = -9.07$, $\beta = -2.62$) and a sustained increase in eutrophication ($Z = 4.00$, $\beta = 1.15$). The NMDS separated two lake groups: one with high nutrients and total coliforms, and another with elevated TDS and conductivity. The PCA identified turbidity, nitrogen, chlorophyll-a, and total coliforms as variables exerting the strongest influence on water variability. The WQI indicated generally poor conditions except in Bacalar Centro and Xul-Ha, which showed fair quality. The highest TSI values occurred in inland systems, except for La Sabana, which exhibited hypereutrophic conditions linked to wastewater inputs. NT–PT ratio indicated nitrogen limitation in most lakes, likely driven by groundwater recharge and low surface runoff. Overall, results demonstrate a progressive decline in water quality and widespread eutrophication across the YP.

Keywords: pollution trend; water quality; eutrophication; limiting nutrient; inland water systems

Check for updates

Academic Editor: Ioannis Panagopoulos

Received: 19 November 2025
Revised: 10 December 2025
Accepted: 16 December 2025
Published: 23 December 2025

Copyright: © 2025 by the authors. Licensee MDPI, Basel, Switzerland. This article is an open access article distributed under the terms and conditions of the Creative Commons Attribution (CC BY) license.

1. Introduction

The Inland water systems (IWS) are experiencing accelerated deterioration at the global scale due to the sustained increase in contaminants, nutrients, and anthropogenic pressures derived from agricultural, urban, and industrial development [1]. Numerous studies assessing water quality in lakes and wetlands, as well as the importance of their ecological functions, resource supply, recreational, and landscape values [2,3], highlight their relevance as key units for aquifer recharge, from which more than 50% of the drinking water consumed worldwide is derived [4].

Climate change represents another critical driver of IWS alteration. The intensification of droughts and the reduction in water levels in lakes and wetlands have promoted progressive nutrient concentration, altered hydrological seasonality, and compromised the function of these systems as infiltration and recharge zones [5,6]. Even IWS located far from population centers exhibit volume losses, enhanced nutrient retention, and biogeochemical disturbances associated with recharge deficits as a consequence of climate change [7,8].

Anthropogenically derived increase in nitrogen (N) and phosphorus (P) triggered widespread eutrophication processes, harmful algal blooms (HABs), and the formation of hypoxic or anoxic zones [9,10]. According to UNEP (United Nations Environment Program), more than 30–40% of lakes in the world exhibit some degree of chronic eutrophication, with an increasing trend since the 1990s [11].

Inland lakes and closed reservoirs are particularly vulnerable due to their low hydrological turnover, which facilitates nutrient accumulation and accelerates the progression toward more eutrophic states [12,13]. In addition, in many developing and developed countries, wastewater discharges, fertilizer-rich agricultural runoff, and livestock inputs far exceed the natural assimilative capacity of aquatic systems [14]. This has reduced the ecological resilience of many lakes, driving them toward ecological tipping points.

Previous studies have shown that large-scale agriculture is responsible for more than 50% of diffuse N and P inputs to lakes and reservoirs [15]. Furthermore, in some tropical systems, increases in TSI exceeding 10 units in less than two decades have been reported, evidencing a rapid advance toward hypereutrophication [16,17].

The Yucatán Peninsula (YP), considered one of the largest underground freshwater reserves in Mexico, exhibits a unique surface hydrology characterized by IWS such as sinkholes (cenotes), flooded caves, large shallow lakes, wetlands, and seasonal water bodies [18–20]. The aquatic environments of this region have been fundamental to the historical development of human populations; for example, the Maya civilization flourished in this area between 2000 BC and 1200 AD [21]. At present, approximately 4.5 million people permanently depend on the surface and groundwater of the peninsula, while an additional 20 million tourists rely on this resource temporarily each year [22].

Currently, the region faces major challenges related to water availability and pollution from diverse sources. Contaminants are dispersed across the land surface or deposited into aquatic systems such as lakes and cenotes, which function as recharge zones for the underlying aquifer [23], driving contamination processes and regional-scale declines in water quality. Wastewater management represents one of the most critical challenges for pollution control, together with the excessive use of fertilizers and pesticides in agricultural and livestock activities, which has intensified in recent decades [24,25]. This is evidenced by the sustained increase in nitrite (>413 $\mu mol \cdot L^{-1}$), ammonium, and coliform bacteria (>1800 $CFU \cdot 100\ mL^{-1}$), as well as by the transition of aquatic environments from oligotrophic and mesotrophic conditions toward eutrophic and hypereutrophic states [26,27]. At present, due to climate change, water availability has been reduced by a decline in the regional moisture balance and alterations in precipitation patterns, thereby promoting a concentration of contaminants and nutrients [28,29]. Recent estimates indicate a mean aquifer recharge of $118 \pm 33\ mm \cdot year^{-1}$ (approximately 10% of total precipitation) during the historical period, whereas projections under climate change scenarios suggest a reduction of 23% (RCP 4.5) and 20% (RCP 8.5), with recharge values decreasing to $92 \pm 40\ mm \cdot year^{-1}$ and $94 \pm 38\ mm \cdot year^{-1}$, respectively [30].

Traditionally, in Mexico, isolated contamination indicators—such as heavy metals, coliforms, and hydrocarbons—have been used to estimate water pollution, water quality, and trophic state [31,32]; however, studies applying integrated water quality indices remain scarce. The comprehensive implementation of indices such as the Water Quality Index

(WQI) and the Carlson Trophic State Index (TSI) has been successfully applied to assess contamination levels in aquatic systems and to identify temporal patterns and degradation rates [33]. These indices allow the synthesis of large datasets derived from multiple variables and indicators into a single value representing contamination levels, which is particularly useful for standardizing values and enabling comparisons across sites and over time.

In this study, using historical data of ten IWS from the YP, obtained from Red Nacional de Monitoreo de la Calidad del Agua (RENAMECA) database (2012–2020) of México, along with additional samplings conducted in 2024, we (a) compared the temporal evolution of water quality and changes in trophic state during the period 2012–2024 as an indicator of long-term water quality trends; (b) provided up-to-date information on water chemistry, microbiological, and limnological data from 29 additional lakes recently sampled in the region; and evaluated spatial patterns of water quality and trophic state changes across the IWS of the Yucatán Peninsula.

2. Materials and Methods

2.1. Study Area

The YP is a karstic plateau composed mainly of limestone, dolomites, and Paleogene evaporites, with a maximum elevation of approximately 250 m in the south-central part of the peninsula and in the Sierrita de Ticul [18]. The hydrology of the YP is characterized by strong subsurface water connectivity and dynamism, and environments such as rivers are practically absent [34]. The IWS in this region displays waters saturated with carbonates and sulfates, although this tendency varies among subregions [19,34]. Climate in this region is classified as tropical—tropical savanna (Aw), characterized by wet summers and dry winters according to the Köppen classification [35]. The mean annual temperature is ~28 °C, and precipitation ranges from ~700 mm in the north to more than 1200 mm in the south [30]. Given its location within natural hurricane trajectories, the peninsula is subject to atypical rainfall events, during which precipitation may reach up to 1200 mm in a single day. It is also highly susceptible to hydrometeorological phenomena such as ENSO and El Niño, which strongly influence the regional moisture balance [36]. Aquatic environments are regionally differentiated within the peninsula according to geomorphology. The northern region, characterized by bare ground, exposed rocks, and high permeability, contains a large number of cenotes—natural sinkholes formed by limestone dissolution that expose the underlying groundwater [18]. In the south-central part of the peninsula, water permeability decreases, likely due to the presence of histosols and gleysols, which promote the development of floodplains and lacustrine environments [20,37].

2.2. Water Sampling and Environmental Parameters Measurements

Data from ten IWS were retrieved from the Red Nacional de Medición de Calidad del Agua (RENAMECA) database for the period 2012–2020 (https://www.gob.mx/conagua/es/articulos/resultados-de-la-red-nacional-de-medicion-de-calidad-del-agua-renameca (accessed on 10 October 2025)). Data were processed using Microsoft Excel and filtered to extract only the variables required to calculate the WQI and the TSI. The variables included chlorophyll-a, fecal coliforms, total coliforms, biochemical oxygen demand (BOD), total nitrogen (TN), total phosphorus (TP), total dissolved solids (TDSs), total suspended solids (TSSs), electrical conductivity, pH, dissolved oxygen, turbidity, and water temperature.

A total of 29 additional inland water systems (IWS) were sampled during April and May 2024 (sampling sites and geographical coordinates are presented in Supplementary Materials Table S1), corresponding to the dry season of the region. Figure 1 shows the geographical location of the 29 sampled IWS. These IWS were closed hydrologi-

cal basins with low or null hydrological connectivity, either surficial or subterranean, and therefore they are prone to eutrophication. Most of the systems were located in the southern part of the YP, along the Caribbean Sea coast, and these lakes were selected because they are the largest lakes in the YP.

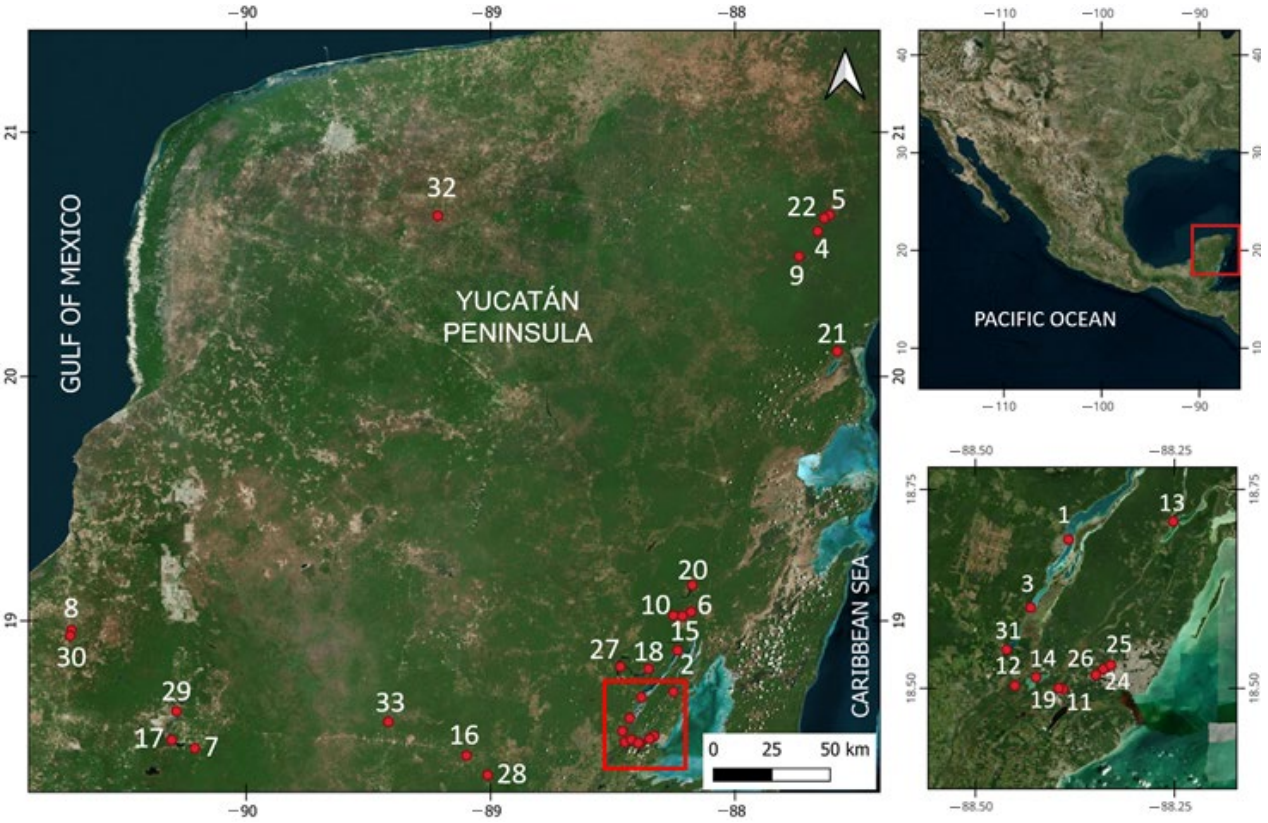


Figure 1. Map of the study area showing the 33 sampling sites across the 29 lakes sampled in 2024 in the Yucatán Peninsula. Bacalar Centro (1), Bacalar Norte (2), Bacalar Sur (3), Campamento Hidalgo (4), Chabela (5), Chacchoben (6), Chan Laguna (7), Chuiná (8), Cobá (9), El Ocho (10), Encantada (11) Guadalupe (12), Guerrero (13), Huay-Pix (14), Lagartija (15), Laguna Om (16), Maravillas (17), Miguel Hidalgo (18), Negra (19), Noh-Bec (20), Nopalitos (21) Punta Laguna (22), Roja Q. Roo (23), Sabana center (24), Sabana North (25), Sabana South (26), San Felipe Bacalar (27), San José de la Montaña (28), Silvituc (29), Xbacab (30), Xul-Ha (31), Yalahau (32), Zoh Laguna (33).

Three sampling sites were established at each lake to ensure sample independence and to provide coverage of both the littoral and central zones of each system. Due to its length (approximately 46 km), Lake Bacalar was subdivided into three basins for independent analysis. Similarly, Lake La Sabana—considered one of the most anthropogenically modified lacustrine systems in the peninsula—was subdivided into three basins, given the spatial variation in trophic state associated with urban development in each of them.

At each sampling site, the following parameters were measured in situ at a depth of 0.5 m: pH, electrical conductivity, and total dissolved solids (TDS) using a portable multiparameter probe (Hanna HI98130; pH: range 0.00–14.00, resolution 0.01; conductivity: range 0.00–20.00 $mS{\cdot}cm^{-1}$, resolution 0.01 $mS{\cdot}cm^{-1}$; TDS: range 0.00–10.00 ppt ($g{\cdot}L^{-1}$), resolution 0.01 ppt ($g{\cdot}L^{-1}$)). Water temperature and dissolved oxygen (DO) were measured using a portable WTW Multi Set 350i meter (temperature: −5.0 to +105.0 °C, resolution 0.1 °C; DO: 0.0–90.0 $mg{\cdot}L^{-1}$ O_2, resolution 0.01 $mg{\cdot}L^{-1}$). Turbidity was determined in nephelometric turbidity units (NTU) using a Thermo Scientific™ Orion™ AQUAfast AQ3010 turbidimeter, which complies with ISO 7027 and provides reliable automatic-range measurements from 0 to 1000 NTU.

Water samples were collected at the same sites and depth (0.5 m) using 1.5 L plastic (polyethylene) bottles previously rinsed with distilled and deionized water. In the field, samples were preserved on ice and protected from direct sunlight until their transport to the Microbiology Laboratory of the Instituto Tecnológico de Chetumal for further analysis. Chlorophyll-a concentration was determined following the standard procedure proposed by Strickland and Parsons (1972) [38], using a Thermo Scientific Genesys UV/Vis 150 spectrophotometer (wavelength range 190–1100 nm, spectral bandwidth 2 nm, and wavelength accuracy ±0.5 nm). Final calculations were performed using the Jeffrey and Humphrey (1975) equation [39], as indicated in Biliani et al. (2025) [40]. Total phosphate was determined using the Hach USEPA1 PhosVer® method with acid persulfate digestion (Standard Methods reference SM 4500 P-E, range 0.06–3.50 $mg \cdot L^{-1}$ P), while total nitrogen was quantified using the Hach low-range persulfate digestion method (reference method 10,071, range 0.5–25.0 $mg \cdot L^{-1}$ N). Both analyses were conducted with a Hach DR 2800 spectrophotometer (wavelength range 340–900 nm).

Biochemical oxygen demand (BOD_5) was measured using the standard five-day method described in Section 5210 of the Standard Methods for the Examination of Water and Wastewater [41]. Total coliform bacteria were determined using 3M Petrifilm plates following the manufacturer's recommended protocol [42].

2.3. Water Quality Index and Trophic State Estimation

We used the WQI proposed by the National Sanitation Foundation to assess water quality in ten IWS sampled between 2012 and 2020, and in twenty-nine systems sampled in 2024. This index is based on ten environmental parameters: temperature (°C), conductivity (mS/cm), pH, TDS (mg/L), oxygen saturation (%), BOD (mg/L), turbidity (NTU), nitrogen (mg N/L), total coliforms, and phosphates (mg PO_4/L). This index was used to estimate the historical and current state of water quality. The percentage of oxygen saturation was calculated using the DOTABLES computational tool [43], which implements the standard solubility equations [44]. These formulations estimate oxygen solubility as a function of temperature, salinity, and atmospheric pressure, following the Practical Salinity Scale (PSS-78). For each sampling point, the measured temperature and conductivity (converted to practical salinity) were entered into DOTABLES to obtain the theoretical dissolved oxygen concentration at 100% saturation. The oxygen saturation percentage was then determined by dividing the measured dissolved oxygen concentration by the theoretical solubility value and multiplying by 100. This approach ensures consistency with internationally accepted protocols for oxygen solubility. For the calculation, an Excel-based calculator provided by the Comisión Nacional del Agua (CONAGUA) of México was used, along with the online tool WQI Calculator for Surface Water Citizen Science (https://www.knowyourh2o.com/outdoor-3/water-quality-index-calculator-for-surface-water, accessed on 24 August 2025) to verify the results [45]. According to the WQI classification, values between 90 and 100 indicate excellent water quality; 70–89 indicate good quality; 50–69 indicate fair quality; 30–49 indicate poor quality; and values below 29 indicate very poor water quality.

The TSI was determined for historical (10 systems sampled from 2012 to 2020) and current data (29 systems sampled in 2024) following the Florida Administrative Code 62-303.200. This index is based on measurements of chlorophyll-a, total nitrogen, and total phosphorus, with calculations available in the report *1996 Water-Quality Assessment for the State of Florida*, Section 305(b) Main Report [46]. The TSI ranges from 1 to 100, with values of 0–29 indicating oligotrophic conditions, 30–59 mesotrophic, 60–69 eutrophic, and 70–100 hypereutrophic conditions. Additionally, the N/P ratio was calculated to determine the limiting nutrient at each IWS.

2.4. Statistical Analysis

To determine the water quality trend in the YP, a Mann–Kendall (M–K) trend analysis and Theil–Sen (T–S) trend analysis were performed to determine the temporal trend of water quality data [47–49]. Prior to this, a Shapiro–Wilk (S–W) normality test was applied to assess data distribution and determine the appropriate analytical method. Theil–Sen trend analysis estimates the median slope of all pairs of points in the time series, allowing the identification of increasing, decreasing, or stable trends. The Shapiro–Wilk (S–W) and Mann–Kendall (M–K) analyses were conducted using OriginPro 2025b, and the Theil–Sen analysis was performed in R 4.5.1 using the trend package. For the trend analyses and to ensure comparability between the 2024 sampling data and the historical records, only the 10 sites with complete historical time series were included.

The M–K analysis is a non-parametric test that evaluates trends in time series values and is calculated using the following equation:

$$Ss = \sum_{i=2}^{n} \sum_{j=1}^{i-1} sgn(xi - xj) \; i \leq n, j \leq n \tag{1}$$

In this equation, *sgn (z)* equals -1 for $z < 0$, 0 for $z = 0$, and +1 for $z > 0$. For a series with random values, it is expected that Ss = 0, and its variance is calculated as follows:

$$Var(Ss) = \frac{\mathrm{n}(\mathrm{n}-1)(2\mathrm{n}+5)}{18} \tag{2}$$

The standardized test statistic is then expressed as follows:

$$Z_S = \frac{\mathrm{Ss} + m_c}{\sqrt{Var(Ss)}} \tag{3}$$

In the formula, $mc = 1$ when Ss < 0, and $mc = -1$ when $Ss > 0$. If the absolute value of Zs exceeds the critical value of the standard normal distribution, the series exhibits an upward or downward trend at a significance level α. For $\alpha = 5\%$, the critical value corresponds to 1.960.

The Theil–Sen analysis allows for the estimation of whether a variable (in this case, water quality and the trophic state of lakes) increases, remains stable, or decreases over a period of time. This analysis calculates the slope of the trend of the variable over time. It is considered a robust method against outliers or data that do not exhibit normality. In this analysis, a positive slope indicates an increasing trend, a negative slope indicates a decreasing trend, and a slope close to zero indicates no clear trend. The formula of the analysis is expressed as follows:

$$B = median\left(\frac{xj - xi}{j - i}\right) \tag{4}$$

where B is the slope of the variable, and xj and xi are the observed values of the time series at time points j and i, respectively. If $B > 0$, the series shows an increasing trend over time, and if $B < 0$, the variable exhibits a decreasing trend over time.

To explore the overall patterns of similarity among the sampled systems with respect to water quality and trophic state, a Non-Metric Multidimensional Scaling (NMDS) was performed using R (version 4.5.1) [50], with the vegan package [51].

To visualize the correlations between environmental variables and sampling sites, as well as possible clustering among the systems, a Principal Component Analysis (PCA) was conducted. This correlation-based analysis uses a simple coefficient to determine the relationship between variables and sampled systems, measuring the strength of associa-

tion and predictive capacity [52]. In hydrological studies, PCA has proven to be useful for identifying the variables that contribute the most to the contamination of aquatic systems [53]. A Multi-Response Permutation Procedure (MRPP) was applied to assess whether the groups formed in the PCA are statistically significant. This non-parametric analysis tests whether two or more groups differ significantly in their multivariate composition based on Euclidean distances, calculating the measure of within-group homogeneity and a *p*-value through permutations. The equation is expressed as follows:

$$A = 1\frac{\delta}{\delta_E} \quad (5)$$

where δ is the observed average within-group distance, and δE is the expected average distance between groups if the members were assigned randomly. With $A = 1$, all elements within the group are identical; $A = 0$, the within-group homogeneity is equal to that expected by chance; and $A < 0$, all elements within a group are less similar than expected by chance.

A non-parametric Monte Carlo test was used to determine which variables contribute most significantly to the formation of these groups [48]. The PCA, MRPP, and Monte Carlo analyses were performed in PCord v.6 [54].

Interpolated maps were used to represent the spatial distribution of WQI and TSI in the study area. We used the kriging algorithm, which weights from surrounding known values to predict unmeasured locations, based on a variogram model. The software Surfer from Golden Software, LLC (www.goldensoftware.com, accessed on 5 September 2025) was used for calculations.

3. Results

3.1. Water Quality and Trophic State Trend Tests

The Shapiro–Wilk test applied to the ten IWS data from 2012 to 2024 revealed significant deviations from normality for both the WQI and the TSI ($p < 0.01$), indicating that the dataset follows a non-parametric distribution. Given the lack of normality, the Mann–Kendall test was employed to identify temporal trends. The results revealed a significant decreasing trend in water quality ($Z = -9.07$, $p < 0.001$) as reflected by the WQI, and a significant increasing trend in trophic state ($Z = 4.00$, $p < 0.001$) according to the TSI.

The robust trend analyses performed using the Theil–Sen estimator revealed contrasting but complementary patterns for the WQI and the TSI over the 2012–2024 period. The WQI showed a significant negative slope ($\beta = -2.62$, $p < 0.001$), indicating a progressive deterioration of water quality, whereas the TSI exhibited a significant positive slope ($\beta = 1.15$, $p < 0.001$), reflecting a progressive increase in the degree of eutrophication. The median of the residuals was close to zero, and the residual standard error of 12.14 indicated a good model fit and high robustness against outliers in the Theil–Sen results for the WQI. The median of the residuals was close to zero, and the residual standard error of 18.48 suggests that, although the temporal trend is clear, there is additional interannual variability in the TSI values.

Figure 2 shows the linear trend estimated through linear regression of water quality, as indicated by the WQI, during the period 2012–2024. With an estimated slope of –3.12 and a decrease of approximately 3.12 units per year, the figure reveals a downward trend in water quality throughout the study period. The negative slope and strong negative correlation (Pearson's r = −0.74647) suggest a progressive deterioration of the physicochemical conditions of the aquatic system, likely associated with contamination processes or increased nutrient loading. The coefficient of determination ($R^2 = 0.55721$) indicates that approximately 55.7% of the variation in WQI is explained by the time factor (year),

showing a considerably strong relationship. The results of this analysis, together with the Mann–Kendall and Theil–Sen trend analyses, indicate that water quality has consistently declined over the study period.

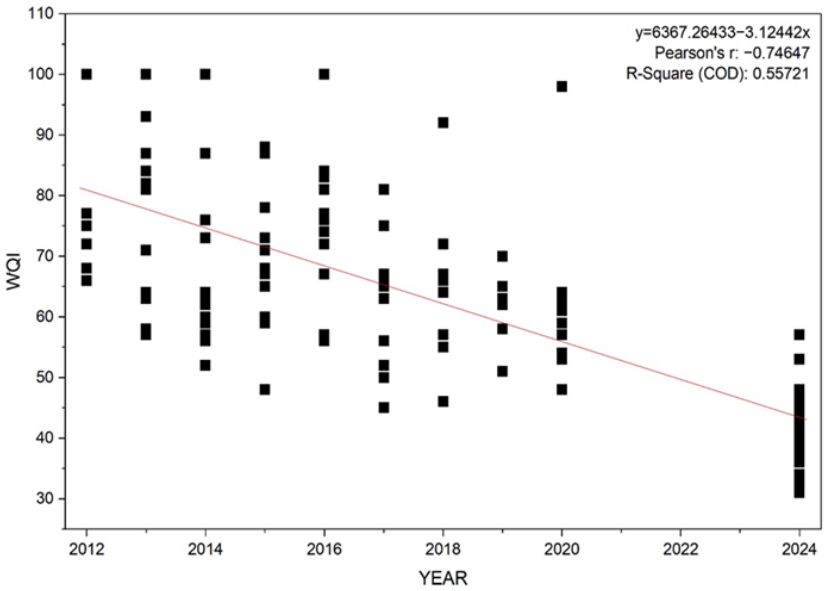


Figure 2. Temporal trend of the Water Quality Index (WQI) between 2012 and 2024. The red line represents the trend, while the black cubes indicate the WQI values obtained for the ten IWS.

Figure 3 shows the linear trend estimated from the TSI data for the period 2012–2024 for the ten IWS. With a slope of 2.17 and an average increase of 2.17 units per year, the figure suggests a rising trend in the level of eutrophication during the analyzed period. The results indicate a progressive trend toward eutrophication, which was also confirmed by the Mann–Kendall and Theil–Sen trend analyses. Although the relationship was not very strong, the positive slope (Pearson's r = 0.4294) and the moderate correlation (R^2 = 0.18438) indicate an increase in the trophic state index (eutrophication) over the study period.

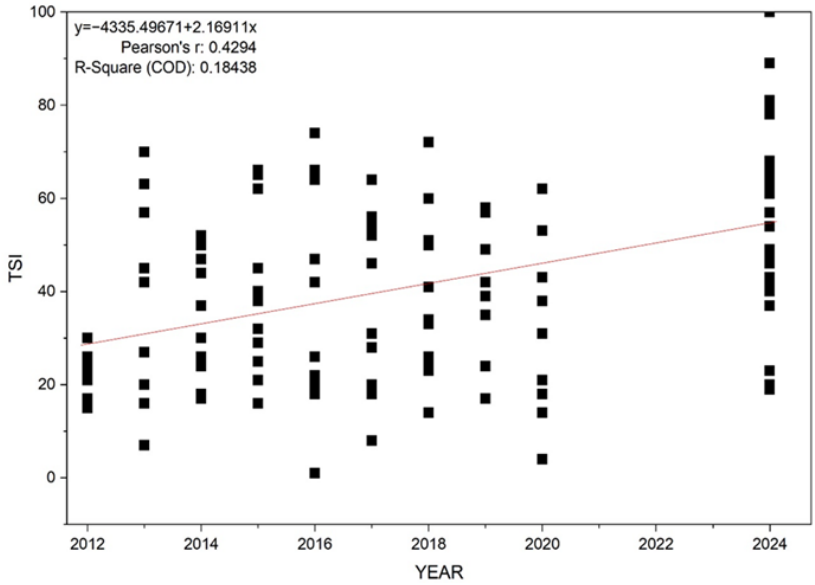


Figure 3. Temporal trend of the Trophic State Index (TSI) between 2012 and 2024. The red line represents the trend, while the black cubes indicate the TSI values obtained for the ten IWS.

3.2. Spatial Analysis of Environmental Variables Associated with Water Quality in 2024

In Table 1, environmental variables measured at each IWS are presented. Data represents the average value at each sampling site. Temperature remained relatively constant in the study area, ranging from 29 °C in Yalahau (northern part of the Peninsula) to 34 °C. Electrical conductivity ranged from 0.38 mS/cm in Maravillas to 19.01 mS/cm in Nopalitos. Lakes Guerrero (8.78 mS/cm) and Roja (13.41 mS/cm), located close to the coast, also exhibited elevated conductivity values. pH ranged from 5.9 in the periurban Lake Sabana center to 8.9 in Yalahau. The TDS ranged from 173 mg/L in Zoh Laguna to 8690 mg/L in Nopalitos. The DO concentrations ranged from a minimum of 2.6 mg/L at the Sabana center to maximum values of 8.8 mg/L and 8.6 mg/L in Zoh Laguna and Bacalar Norte, respectively. The BOD ranged from 1.6 mg/L in Xul-Ha to a maximum of 23.6 mg/L in Nopalitos. Notably, this latter value is characteristic of systems potentially impacted by wastewater discharges, nearing the threshold of 30 mg/L. The La Sabana North system, which receives treated effluent from a nearby wastewater treatment plant adjacent to the city of Chetumal, showed a BOD of 13.2 mg/L—consistent with systems affected by treated discharges. Other systems also exhibited high BOD values, including Chabela (11.7 mg/L), Laguna Om (14.7 mg/L), Lagartija (10.5 mg/L), and Zoh Laguna (10.7 mg/L). Turbidity reached its highest levels in Chacchoben (429.7 NTU), El Ocho (349.5 NTU), and Sabana North (239.3 NTU), while the lowest values were recorded in Bacalar Sur (1.65 NTU), Nopalitos (1.217 NTU), Encantada (0.793 NTU), and Laguna Negra (0.953 NTU). Total nitrogen (TN) concentrations were highest in Chacchoben (29.167 mg N/L), El Ocho (17.3 mg N/L), and Sabana North (13.5 mg N/L), while the lowest levels were observed in Bacalar Centro (0.3 mg N/L), Guadalupe (0.4 mg N/L), and Xul-Ha (0.667 mg N/L). Phosphate (PO_4^{3-}) concentrations peaked in Sabana North (3.21 mg PO_4/L), Chacchoben (0.91 mg PO_4/L), and San José de la Montaña (0.883 mg PO_4/L). The lowest phosphate levels were found in Chuina (0.29 mg PO_4/L), Xbacab (0.28 mg PO_4/L), and Silvituc (0.283 mg PO_4/L). Chlorophyll-a concentrations showed a wide range across systems, from very high values in Sabana North (716.41 mg/m^3), Chacchoben (673.61 mg/m^3), and El Ocho (576.95 mg/m^3), to minimal concentrations in Guadalupe (0.3 mg/m^3), Milagros (0.38 mg/m^3), and Xul-Ha (0.21 mg/m^3). Total coliforms also varied considerably among the systems, with the highest counts recorded in Sabana North and Centro (270,000 and 198,000 CFU/100 mL, respectively), indicating high levels of contamination. The lowest counts were observed in Miguel Hidalgo and Xul-Ha, with 700 and 500 CFU/100 mL, respectively.

Table 1. Physiochemical parameters of the IWS at the Yucatán Peninsula during 2024.

Lake	T°C	Con. (mS/cm)	pH	TDS (mg/L)	OD (mg/l)	OS (%)	BOD (mg/L)	Turb (NTU)	TN (mgN/L)	PO (mgPO4/L)	Chl-a (mg/m^3)	TC (CFU/100 mL)
BAC	31	2.667	6.8	1337	7.8	105	1.8	2.04	0.3	0.4	0.4	10,800
BAN	31	3.053	7	1527	8.6	115.8	3.9	3.69	1.5	0.47	0.47	1400
BAS	30	2.433	6.5	1220	5.7	75.4	5.1	1.65	0.433	0.373	0.26	7200
CAH	30	1.18	8.4	5930	5.8	76.72	9.4	13.04	0.933	0.437	15.52	11,000
CHA	30	1.38	8.5	6080	6.6	87.3	11.7	2.625	0.95	0.655	2.07	9800
CAC	32	0.803	7.9	400	7.5	102.7	6.2	429.7	29,167	0.91	673.61	8400
CHL	34	0.5	7	250	5.6	79.32	3.5	5.137	1.833	0.293	18.85	6333.3
CHU	33	0.74	7.6	370	5.4	75.21	4.6	11.34	0.833	0.29	11.9	3066.7
COB	30	1.38	7.7	6890	7.6	100.5	7	7.25	1.667	0.603	6.15	29,400
ENC	32	3.32	6.8	1667	6.2	84.93	6.45	0.793	2.5	0.36	1.8	9000
GUA	31	3.26	6.8	1617	6.4	86.14	6.3	1.707	0.4	0.367	0.3	2300
GUE	31	8.7825	6.7	4380	9.6	129.2	3.6	2.975	2.6	0.325	0.54	8000
LAG	32	1.653	7.4	827	6.3	86.3	10.5	41.78	3.5	0.7	56.81	12,133.3

Table 1. *Cont.*

Lake	T°C	Con. (mS/cm)	pH	TDS (mg/L)	OD (mg/l)	OS (%)	BOD (mg/L)	Turb (NTU)	TN (mgN/L)	PO (mgPO4/L)	Chl-a (mg/m^3)	TC (CFU/100 mL)
LNO	34	0.38	7.8	190	6.6	93.48	5.1	26.37	4.333	0.39	39.65	11,400
LOM	33	0.41	7.2	207	8	111.4	14.7	3.583	1.5	0.357	14.2	15,600
MIH	33	0.73	7.7	367	7.7	107.2	6	14.97	2.433	0.46	16.36	700
MIL	30	3.31	7	1653	6.633	87.7	5.2	3.757	2	0.4	0.38	1300
NEG	30	3.277	6.9	1640	7.5	99.21	3.1	0.953	2.2	0.37	1.4	4200
NOB	32	2.463	7.3	1230	6.2	84.93	3.15	2.363	1	0.37	1.31	3666.7
NOP	30	19.01	8.4	8690	7.9	104.5	23.6	1.217	0.167	0.667	25.6	25,200
OCH	32	0.423	8.3	210	7.8	106.9	6.3	349.5	17.3	1.63	576.95	28,000
PUL	30	1.42	8.4	710	5.7	75.4	5.2	1.71	4.367	0.44	2.5	16,800
ROJ	30	13.41	7.2	6697	6.6	87.3	8.4	5.083	1.4	0.387	1.99	4000
SAC	31	3.9	5.9	1960	2.6	34.85	8.4	6.93	1.8	0.67	8.4	198,000
SAN	33	3.32	7.5	1240	5.8	80.22	13.2	239.3	13.5	3.21	716.41	270,000
SAS	34	4.37	6.4	2150	4.9	69.8	8.4	2.23	3.9	0.52	3.58	19,800
SFB	31	0.628	7	314	6.9	92.87	3.7	9.842	1.52	0.394	18.06	4980
SIL	34	0.507	7.3	253	7.4	104.8	6	15.97	1.867	0.283	24.67	9066.7
SJM	31	0.497	6.9	250	6.4	86.14	6.4	5.41	1.833	0.883	11.57	19,800
XBA	32	4.273	7.2	2137	5.2	71.23	6.5	35.74	1.5	0.28	52.65	9200
XUH	30	2.407	6.5	1200	7.6	100.5	1.6	2.45	0.667	0.323	0.21	500
YAL	29	2.27	8.9	1140	5.7	74.12	3.8	14.02	2.267	0.387	15.64	22,400
ZOL	34	0.35	7.5	173	8.8	124.7	10.7	9.73	2.167	0.4	10.87	6766.7

Abbreviations are as follows: Bacalar Centro (BAC), Bacalar Norte (BAN), Bacalar Sur (BAS), Campamento Hidalgo (CAH), Chabela (CHA), Chacchoben (CAC), Chan Laguna (CHL), Chuiná (CHU), Cobá (COB), Encantada (ENC), Guadalupe (GUA), Guerrero (GUE), Lagartija (LAG), Maravillas (LNO), Laguna Om (LOM), Miguel Hidalgo (MIH), Milagros (MIL), Negra (NEG), Noh-Bec (NOB), Nopalitos (NOP) El Ocho (OCH), Punta Laguna (PUL), Roja Q. Roo (ROJ), Sabana center (SAC), Sabana North (SAN), Sabana South (SAS), San Felipe Bacalar (SFB), Silvituc (SIL), San José de la Montaña (SJM), Xbacab (XBA), Xul-Ha (XUH), Yalahau (YAL), Zoh Laguna (ZOL).

The NMDS on the first axis grouped systems exhibiting high turbidity, and concentration of nitrogen, chlorophyll-a, and total coliforms. Axis 2 was associated with systems with higher levels of TDS and electrical conductivity (Figure 4). Systems such as Bacalar, Xul-Ha, Noh-Bec, Chabela, Negra, Encantada, Milagros, Guadalupe, and Punta Laguna clustered closely, primarily due to high values of TDS and conductivity and low nutrient levels (Figure 4, yellow group). Systems with higher temperature and dissolved oxygen concentrations—such as Miguel Hidalgo, Chuina, Cobá, Lagartija, San Felipe Bacalar, Zoh Laguna, Chan Laguna, San José de la Montaña, and Laguna Om (Figure 4, red group)—were also positioned closely together. These systems were likewise characterized by low nutrient concentrations. Although Lagartija and Maravillas were located near this group, they exhibited comparatively higher concentrations of nitrogen, chlorophyll-a, and total coliforms (Figure 4). Systems such as La Sabana North, El Ocho, and Chacchoben were grouped apart, primarily due to their elevated levels of nitrogen, phosphate, chlorophyll-a, total coliforms, and turbidity. Conversely, Nopalitos emerged as a distinctly different system due to its extremely high conductivity, TDS values, elevated BOD, and high total coliform counts (Figure 4).

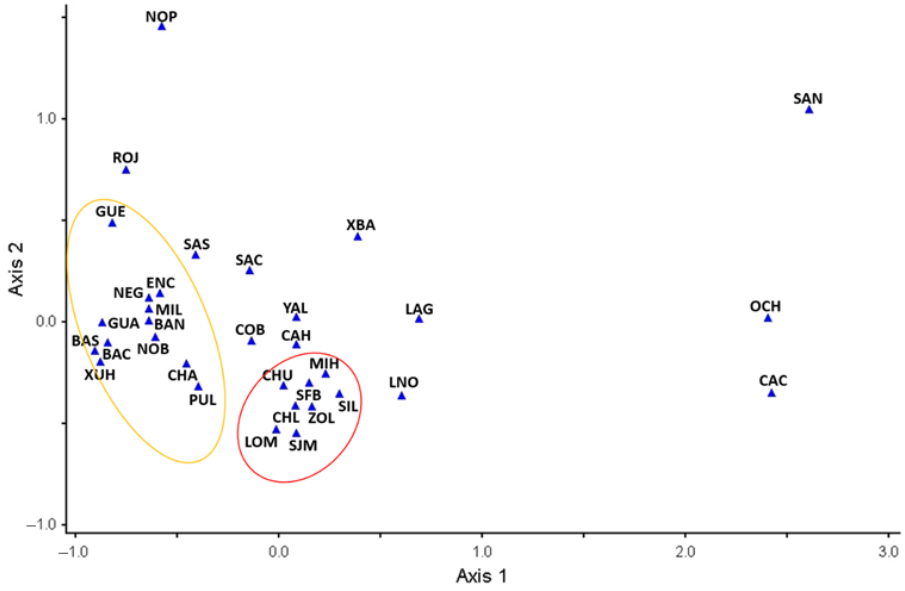


Figure 4. Non-metric Multidimensional Scaling (NMDS) showing the similarity among the systems. Abbreviations are the same as in Table 1.

The PCA biplot based on PC1 and PC2 accounted for 65.82% of the total data variance (Figure 5). The PC1 explained 42.74% of the variance and was strongly associated with turbidity, nitrogen, and chlorophyll-a, revealing that these variables are the most influential in the data set. PC2 explained 23.08% of the variance, with temperature being the main variable influencing this component.

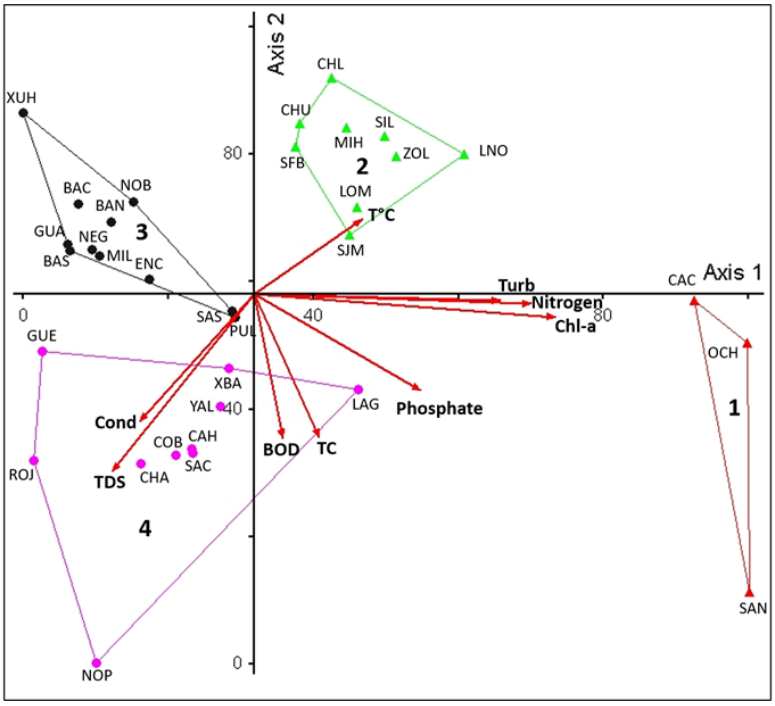


Figure 5. Principal Component Analysis (PCA) of the sampled systems, showing their distribution according to the relationship among environmental variables: Temperature (T°C), Conductivity (Cond), total dissolved solids (TDS), biochemical oxygen demand (BOD), turbidity (Turb), Nitrogen, Phosphate, chlorophyll-a (Chl-a) and total coliform (TC). Abbreviations of the site are the same as in Table 1.

The MRPP analysis showed that all groups identified in the PCA were statistically different, with *p*-values below 0.001 in all cases. The Monte Carlo test showed that for Group 1, the main contributing variables were chlorophyll-a, nitrogen, phosphates, and turbidity; for Group 2, temperature; and for Group 4, conductivity was the most influential variable (Figure 3). For Group 3, no significant statistical relationship was found with any of the measured variables.

3.3. Spatial Water Quality and Trophic State of the Yucatán Peninsula During 2024

Water quality ranged from poor to fair. Only two systems exhibited fair quality (Bacalar Centro and Xul-Ha), while the remaining systems showed poor quality (Table 2). Lake La Sabana displayed differences in water quality among its three sub-basins. Sabana South showed better quality compared to the other two sites. Similarly, Bacalar exhibited variability in water quality among its subsystems, with the best quality observed in the central area near the city of Bacalar. Most systems with poorer quality were characterized by high levels of total coliforms, chlorophyll-a, and nutrients (Table 2). In contrast, systems with poor quality were also characterized by high conductivity, elevated temperature, and high total dissolved solids, the latter primarily due to the elevated carbonate content in their waters.

Table 2. Water Quality Index (WQI), Trophic State Index (TSI), and nitrogen-to-phosphorus ratio of the inland water systems evaluated in the Yucatán Peninsula. Abbreviations are the same as in Table 1.

Lake	WQI	Water Quality	TSI	Trophic State	N:P Ratio	Limiting Nutrient
BAC	53	FAIR	19	Oligotrophic	2.3	Nitrogen
BAN	46	POOR	37	Mesotrophic	9.77	Nitrogen
BAS	44	POOR	20	Oligotrophic	3.55	Nitrogen
CAH	36	POOR	57	Mesotrophic	6.54	Nitrogen
CHA	34	POOR	43	Mesotrophic	4.44	Nitrogen
CAC	34	POOR	100	Hypereutrophic	98.08	Phosphorus
CHL	47	POOR	62	Eutrophic	23.8	Balanced
CHU	45	POOR	54	Mesotrophic	8.59	Nitrogen
COB	38	POOR	57	Mesotrophic	8.45	Nitrogen
OCH	33	POOR	100	Hypereutrophic	32.48	Phosphorus
ENC	43	POOR	49	Mesotrophic	21.25	Balanced
GUA	43	POOR	20	Oligotrophic	3.34	Nitrogen
GUE	45	POOR	40	Mesotrophic	24.48	Balanced
MIL	44	POOR	37	Mesotrophic	15.3	Balanced
LAG	39	POOR	78	Hypereutrophic	15.3	Balanced
LOM	39	POOR	61	Eutrophic	13.05	Balanced
LNO	42	POOR	81	Hypereutrophic	32.81	Phosphorus
MIH	45	POOR	66	Eutrophic	15.95	Balanced
NEG	48	POOR	46	Mesotrophic	18.19	Balanced
NOB	48	POOR	40	Mesotrophic	8.27	Nitrogen
NOP	32	POOR	42	Mesotrophic	0.77	Nitrogen
PUL	41	POOR	62	Eutrophic	30.37	Phosphorus
ROJ	39	POOR	47	Mesotrophic	11.08	Balanced
SAC	37	POOR	89	Hypereutrophic	8.22	Nitrogen
SAN	31	POOR	100	Hypereutrophic	12.86	Balanced
SAS	39	POOR	79	Hypereutrophic	22.95	Balanced
SFB	46	POOR	63	Eutrophic	11.65	Balanced
SJM	41	POOR	62	Eutrophic	8.05	Nitrogen

Table 2. *Cont.*

Lake	WQI	Water Quality	TSI	Trophic State	N:P Ratio	Limiting Nutrient
SIL	43	POOR	64	Eutrophic	26.33	Balanced
XBA	42	POOR	68	Eutrophic	18.88	Balanced
XUH	57	FAIR	23	Oligotrophic	6.31	Nitrogen
YAL	42	POOR	64	Eutrophic	17.94	Balanced
ZOL	40	POOR	61	Eutrophic	15.88	Balanced

The trophic state of IWS ranged from 19 (oligotrophic) to 100 (hypereutrophic). Systems exhibiting good water quality also showed oligotrophic conditions, with Bacalar Centro standing out as the site with the best water quality and the lowest trophic index (Table 2). Bacalar Centro and Sur were classified as oligotrophic, whereas Bacalar Norte was mesotrophic, indicating a higher nutrient input in the northern part of the system. In contrast, all three sites within the La Sabana system (North, Center, and South) were classified as hypereutrophic (Table 2).

The interpolated map of WQI shows that environments in the central and western portions of the YP, and in the Bacalar hydrological corridor located in the south, exhibit better water quality. In this study, we included only lake-type environments, and, therefore, we could not evaluate the potential influence of industrial pig farms in the northern part of YP, affecting mostly cenotes and subterranean waters. Environments located along the Caribbean Sea coast, close to large urban centers such as Cancún, Playa del Carmen, and Tulum in the touristic regions, display lower values of WQI, indicating overall bad water quality. The TSI interpolated map shows mostly homogeneous trophic conditions in the center of the YP, but higher values were observed in the agricultural zones of southern Campeche and Quintana Roo, and in lakes close to urban centers such as Chetumal. Interestingly, along the Caribbean Sea coast, TSI values were relatively low, but this can be related to the strong connectivity of lakes with the aquifer.

It is important to note that systems with a eutrophic or hypereutrophic state do not necessarily exhibit poor water quality. For instance, Laguna Maravillas was classified as hypereutrophic but showed higher water quality, as measured by the WQI, than other systems classified as eutrophic or hypereutrophic (Table 2). This is because the system has high concentrations of nutrients and chlorophyll-a, but low levels of total coliforms and biochemical oxygen demand—both indicators of contamination that are given greater weight in the WQI assessment.

4. Discussion

4.1. Temporal Trends of Water Quality (2012–2024)

The Mann–Kendall and Theil–Sen trend analyses show downward trends of water quality and an increasing trend in trophic state over a decade, indicating a consistent process rather than short-term fluctuations. Despite the lack of monitoring data for 2021–2023, resulting from the suspension of field campaigns during the COVID-19 pandemic, the 2024 dataset confirms the progression of these trends. They are consistent with the cumulative anthropogenic pressures in the region, closely linked to population growth (from 4.1 million in 2020 to 5.1 million in 2024) and the development of large-scale infrastructure projects such as Felipe Carrilo Puerto airport, industrial farms, and Tren Maya that have intensified land-use change and ecosystem disturbance [18].

Tourism and increased concentrations of contaminants also show a correlation. It was estimated that there was an arrival of 27 to 18.4 million visitors every year in YP, evidencing unsustainable practices in the aquatic environment itself, such as sun blockers and repellents (in lakes and cenotes), and increasing the volume of wastewater [55–57].

This phenomenon has been previously reported in urban cenotes close to the largest cities in the region, such as Cancun and Mérida, in cenotes Xbatun, Xcanche, Kankirische, and Yokdzonot, all of them located within the tourist region. In all these cenotes, total coliform colonies were too numerous to count, fecal coliforms exceeded 439 CFU 100 mL^{-1}, and Enterococcus levels were higher than 252 CFU 100 mL^{-1}, and with elevated nutrient concentrations (nitrate >70.61 mg L during peak tourist seasons [55,57].

The cultivated area has also increased considerably. According to INEGI, approximately 14.3% of the total surface area of the YP is used for agriculture, and in most areas, agrochemicals and fertilizers are applied [58]. These compounds have been detected in groundwater systems and have dispersed at the regional scale [59]. The intensification of agricultural production, particularly in the state of Quintana Roo, through the cultivation of sugarcane (362.99 km^2) and maize (436.11 km^2) [60], has led to an increased use of agrochemicals that are dispersed through natural runoff and artificial agricultural channels [61]. These flows ultimately discharge into closely located IWS, or through subterranean connectivity to the Río Hondo or the Bacalar–Bahía de Chetumal hydrological corridor, which encompasses some of the most important aquatic systems in the southern YP in terms of biodiversity and economic development [19].

One of the main sources of contaminants in the region is the limited sanitation infrastructure and poor wastewater treatment. This is an endemic problem in Latin America, where only about 20 percent of wastewater receives adequate treatment [25]. In the urban areas of the peninsula, the absence of surface drainage associated with its predominantly flat topography—over 90 percent of the territory lies below 200 m in elevation—limits the natural flow of contaminants [62], favoring the accumulation in hydrological basins and thus, the decline of regional water quality and trophic state. Lake La Sabana (in the southern YP, next to the Chetumal city) is currently considered one of the most anthropogenically altered environments. It has been reported that total coliform concentrations exceeding >50,000 MPN 100 mL^{-1} and fecal coliform concentrations above >18,000 MPN 100 mL^{-1} occur during the rainy season. On this lake, the continuous discharge of partially treated wastewater has modified the trophic state over the last years, shifting it from mesotrophic to hypereutrophic. Because of nutrient availability, an exponential proliferation of invasive species such as *P. stratiotes* and *E. crassipes* has occurred since 2018, not previously observed in YP. This event marked a precedent for the associated consequences of the alterations in trophic structure. Currently, similar patterns are being replicated in the northern part of the YP, such as in Akumal and Tankah cenote, where poor wastewater management has led to aquifer contamination and changes in phytoplankton composition [63].

Climatic factors also appear to play an important role in water quality deterioration. Variability in precipitation—ranging from prolonged droughts to atypical or extreme rainfall events [64,65]—can increase contaminant loads over short time periods. During 2020, for example, a short-term brownification event occurred in the mostly oligotrophic Lake Bacalar [66]. Brownification appeared to be multifactorial and related to intense rainfall and increased nutrient inputs from subterranean and surface runoff (related to deforestation and land use change. This brownification altered the trophic state of the system and produced effects on the structure and functioning of the biological communities within the lake [19].

In the near future, brownification events may be more common in oligotrophic IWS of the region, as increases in global temperature and rainfall budget are expected. Steady global surface warming from 1973 to 2022, but an increased warming rate after 1990 has direct implications for these environments [67]. Rising temperatures in shallow surface water bodies promote harmful algal blooms, reduce dissolved oxygen concentrations, and con-

centrate pollutants through evaporation, therefore promoting eutrophication processes [68]. This can generate positive feedback loops, where eutrophic conditions further accelerate ecosystem degradation and reduce ecological resilience.

The results of the present study are consistent with those obtained in other tropical areas, in the Hirakud Reservoir in India [69], where turbidity, dissolved oxygen, phosphate, water transparency, and electrical conductivity were identified as the main variables explaining the variability of chlorophyll-a and, consequently, the evolution of the eutrophication process. Similarly, in the IWS of the YP, the intensification of eutrophication is closely associated with the progressive deterioration of physicochemical water conditions, particularly in systems subjected to agricultural runoff, such as Miguel Hidalgo and Silvituc, to continuous urban discharges, such as La Sabana and Bacalar, and to a reduced capacity for hydrological renewal, such as Lagartija and Chacchoben. These systems exhibit favorable conditions for the accumulation of nutrients and organic matter, which promotes algal proliferation and the transition toward higher trophic states.

In an analogous manner, in the karstic basin of the Río Grande de Comitán–Lagos de Montebello, Chiapas, it has been documented that water quality remains relatively good in areas with conserved forest cover and land-use regulations, whereas in the middle basin, a deterioration has been observed associated with both inadequately treated urban discharges and diffuse agricultural pollution. In both contexts, the shallow nature of the water bodies, the surface connectivity among lakes, and the high permeability of the karstic substrate act as efficient mechanisms for the rapid propagation of contaminants at the basin scale, significantly increasing the vulnerability of aquatic systems to anthropogenic pressures [32].

4.2. State in the Yucatán Peninsula During 2024

Environmental variables measured in 2024 reveal high physicochemical and microbiological heterogeneity among the IWS of the YP, reflecting a gradient of ecological conditions ranging from well-preserved environments to heavily impacted water bodies. The lowest values of the WQI were observed along the eastern Caribbean coast, adjacent to the Caribbean Sea. This pattern may be related to the accelerated population growth (both residents and visitors), linked with the economic development of the region. There, the establishment of housing areas was faster than the establishment of sanitary services. Consequently, large areas of the cities and towns lack efficient wastewater treatment plants. The population concentrated mainly in Caribbean coastal cities such as Cancún, Playa del Carmen, Tulum, and Chetumal amounted to approximately 874,000 inhabitants in the year 2000. By 2020, the estimated population in these cities had reached about 1,800,000 inhabitants, representing more than a twofold increase over two decades [70,71].

The highest WQI values (Figure 6A)—indicative of better water quality—are recorded in the central and western portions of the peninsula, where the touristic and industrial development tends to be lower compared with other zones of the Peninsula. This is a zone with mostly shallow soils with exposed rocks, precluding large-scale agriculture and farming. However, it is important to note that we only sampled surface waters (primarily lakes), and, therefore, the potential influence of large-scale pig farming, which affects groundwater, was not taken into account.

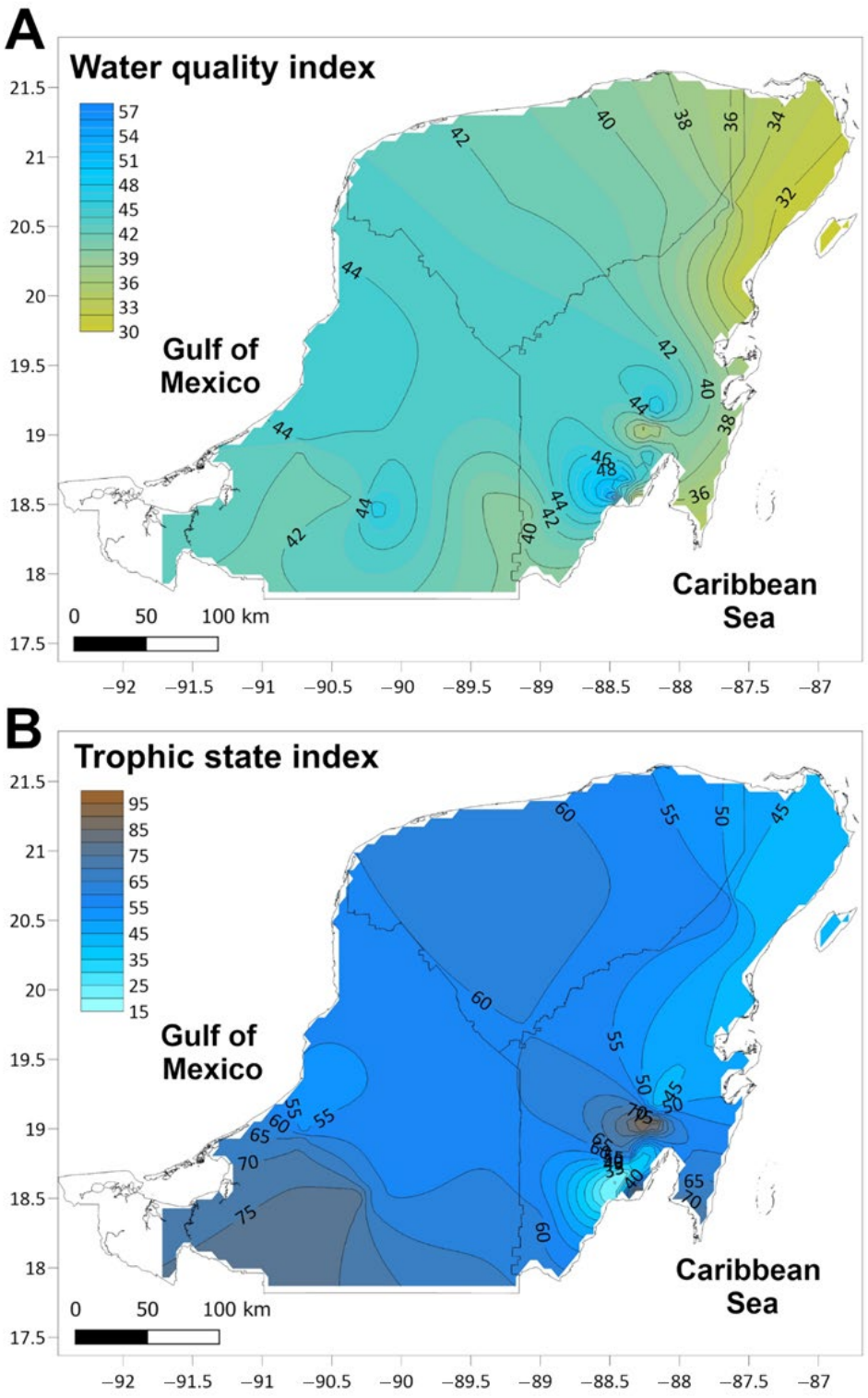


Figure 6. Spatial distribution of the (**A**) Water Quality Index and (**B**) Trophic State Index in inland water bodies of the Yucatán Peninsula.

In contrast, the pattern observed for the TSI (Figure 6B) shows higher values toward the southern and southwestern regions of the peninsula, indicating mesotrophic to eutrophic conditions compared to the northern and northeastern zones, where lower values reflect more oligotrophic states. This variation could be explained by nutrient accumulation in closed basin systems or those with more prolonged water residence [72,73], as well as by the input of organic matter derived from natural or anthropogenic processes [25]. Northern YP lakes, mostly connected by the aquifer, tend to be more hydrologically dynamic, because

of the subterranean flow, compared with the floodplains, non- or partially connected with the aquifer characteristic of the southern YP.

The comparison between both indices reveals an inverse relationship: areas with low water quality (reduced WQI) tend to coincide with zones exhibiting higher trophic states (elevated TSI). However, both indices should be analyzed separately, since eutrophic conditions do not necessarily imply poor water quality [26,74]. For example, Lake Bacalar exhibits oligotrophic conditions and fair water quality, whereas Guadalupe and Chabela, which display oligotrophic and mesotrophic conditions, respectively, have poor water quality.

The N–P ratio showed that nitrogen-limited systems corresponded mainly to oligotrophic–mesotrophic IWS, whereas nutrient-balanced systems are generally eutrophic (Table 2). Hypereutrophic systems tend to exhibit phosphorus limitation, likely due to phytoplankton's uptake. In the case of Sabana North, despite showing high chlorophyll-a concentrations, indicative of high primary productivity, the system maintains a balanced nutrient ratio, possibly due to the presence of a nearby wastewater discharge of large amounts of nutrients. On the other hand, high nitrogen levels corresponded to elevated chlorophyll-a concentrations, reflecting the role of nitrogen in driving primary productivity in the aquatic systems [75].

Most lakes exhibited nitrogen limitation (N–P < 16), which is likely associated with the fact that, during the dry season, groundwater—characterized by low nitrogen concentrations due to denitrification processes—constitutes their primary source of water. Additionally, the limited surface runoff during this period further reduces external nitrogen inputs [18,76]. In contrast, the phosphorus-limited lakes identified in this study likely receive higher nutrient inputs—such as from agricultural fertilizers, wastewater discharges, or soil disturbances—or exhibit significant internal phosphorus retention due to organic-rich sediments [25]. Lakes located in the northern Bacalar region, and its surroundings tend to be nitrogen-limited, whereas several lakes in the central-southern region may be related to variations in land use (agriculture, urbanization, and tourism), hydrological connectivity, and water residence time, as well as local geological composition [77]. Typically, oligotrophic lakes tend to be nitrogen-limited, while eutrophic systems are more often phosphorus-limited [78]. Nitrogen-limited lakes may favor N-fixing cyanobacteria, whereas phosphorus-limited lakes exhibit restricted algal biomass due to limited P availability [79]. Balanced systems, in turn, may be more susceptible to eutrophication if external nutrient inputs increase. Previous studies have reported that the Bacalar system is predominantly nitrogen-limited due to its karstic geology and low nitrogen inputs [19,80]. Conversely, lakes located near agricultural or urbanized areas, such as Chacchoben, El Ocho, and Maravillas, show higher phosphorus availability.

The reviewed studies consistently agree that nutrient loads—particularly total nitrogen (TN) and total phosphorus (TP)—constitute one of the main factors controlling water quality in surface water systems [81,82]. Numerous investigations have demonstrated that elevated TP and NH_3–N concentrations clearly reflect the dominant influence of agricultural activities, whereas physical factors such as topography, geomorphology, and the intensity of human activities modulate the spatial patterns of degradation [53,83]. Studies indicate that water quality exhibits marked seasonal variability, mainly associated with increases in TN and TP [82].

Likewise, approaches based on predictive modeling and machine learning techniques confirm that total phosphorus, ammoniacal nitrogen, and dissolved oxygen are the most robust key parameters for explaining and predicting the behavior of the Water Quality Index (WQI), achieving high levels of accuracy [84]. These findings reinforce the central role of nutrients and oxygenation as direct determinants of the ecological status of aquatic

systems. In addition, Principal Component Analysis-based studies reveal that water temperature and dissolved oxygen concentration respond rapidly to changes in other physicochemical variables, particularly in small-scale catchments with rapid hydrological response, factors that may explain why larger systems tend to exhibit better water quality than smaller ones [53].

Taken together, these studies demonstrate that water quality emerges as the result of a complex interaction between anthropogenic drivers (agriculture, effluent discharges, and land use) and physical and hydrometeorological factors (temperature, hydrological dynamics, and geomorphology), highlighting the need for integrated approaches to water quality monitoring and management.

5. Conclusions

The temporal analyses conducted in this study revealed a consistent and significant deterioration of water quality in the IWS of the YP between 2012 and 2024, accompanied by a progressive intensification of eutrophication. The spatial analysis further showed a generalized degradation of water quality across the peninsula, likely associated with infrastructure development, agroindustrial expansion, population growth, and increasing tourism pressure. Eutrophication currently represents one of the major environmental challenges for tropical aquatic systems in the region. Critical cases such as Lake La Sabana—characterized by poor water quality and hypereutrophic conditions driven by wastewater discharges—highlight the urgent need to protect water bodies that still maintain good ecological integrity through preventive and adaptive management strategies.

Although multivariate tools and integrative indices, such as the NSF-WQI, proved effective for differentiating systems according to their degree of degradation, this study has several limitations. The absence of monitoring data during 2021–2023 restricted the detection of short-term interannual variability for this period, and the spatial assessment was limited to surface lacustrine environments, excluding cenotes and subterranean systems, which constitute essential components of the karst hydrology of the peninsula. Moreover, the 2024 dataset reflects only dry-season conditions and, therefore, does not capture the nutrient pulses and hydrological dynamics characteristic of the rainy season. In this context, the findings underscore the need to strengthen continuous monitoring programs by integrating advanced technologies such as remote sensing and early-warning systems, particularly in areas experiencing high tourism pressure or rapid urban expansion. Despite these limitations, the results highlight the urgent need to implement an integrated management strategy for the aquatic systems of the YP, supported by long-term monitoring efforts in both time and space, in order to ensure water of acceptable quality for ecological integrity and human development in the near future.

Supplementary Materials: The following supporting information can be downloaded at: https://www.mdpi.com/article/10.3390/hydrology13010006/s1. Table S1 Data from the lake sampled in 2024.

Author Contributions: Conceptualization, P.H.-H. and S.C.; methodology, P.H.-H. and N.O.C.-Z.; software, S.C. and J.R.B.-C.; validation, L.M.-G., L.Q.C.-P., J.R.B.-C., L.M.-O. and C.M.H.; formal analysis, P.H.-H., S.C. and J.R.B.-C.; investigation, P.H.-H. and N.O.C.-Z.; resources, S.C.; data curation, P.H.-H. and S.C.; writing—original draft preparation, P.H.-H. and S.C.; writing—review and editing, P.H.-H., L.M.-G., L.Q.C.-P., S.C., N.O.C.-Z., J.R.B.-C., L.M.-O. and C.M.H.; visualization, S.C.; supervision, S.C.; project administration, S.C.; funding acquisition, S.C. All authors have read and agreed to the published version of the manuscript.

Funding: Tecnológico Nacional de México (TecNM) project number 23329.25-P and SECIHTI, through fellowship number 1007683, awarded to the first author, supported this work.

Data Availability Statement: Temporal data presented in this study are available in Resultados de la Red Nacional de Medición de Calidad del Agua (RENAMECA) at https://www.gob.mx/conagua/es/articulos/resultados-de-la-red-nacional-de-medicion-de-calidad-del-agua-renameca. These data were derived from the following resources available in the public domain: Resultados RENAMECA https://files.conagua.gob.mx/aguasnacionales/TODOS%20LOS%20MONITOREOS.xlsb, all accessed on 10 October 2025.

Acknowledgments: We thank the Instituto Tecnológico de Chetumal for providing the laboratory space and equipment used for analysis. Special thanks to the biology undergraduate students Rodrigo Ek-Ceballos, Ilce Cosgalla-López, and Sugeyly May-Espinosa, who contributed to the sampling and laboratory analysis.

Conflicts of Interest: The authors declare no conflicts of interest.

References

1. Dudgeon, D.; Arthington, A.H.; Gessner, M.O.; Kawabata, Z.-I.; Knowler, D.J.; Lévêque, C.; Naiman, R.J.; Prieur-Richard, A.-H.; Soto, D.; Stiassny, M.L.J.; et al. Freshwater Biodiversity: Importance, Threats, Status and Conservation Challenges. *Biol. Rev. Camb. Philos. Soc.* **2006**, *81*, 163–182. [CrossRef] [PubMed]
2. Vári, Á.; Podschun, S.A.; Erős, T.; Hein, T.; Pataki, B.; Iojă, I.-C.; Adamescu, C.M.; Gerhardt, A.; Gruber, T.; Dedić, A.; et al. Freshwater Systems and Ecosystem Services: Challenges and Chances for Cross-Fertilization of Disciplines. *Ambio* **2022**, *51*, 135–151. [CrossRef] [PubMed]
3. Wong, C.P.; Jiang, B.; Bohn, T.J.; Lee, K.N.; Lettenmaier, D.P.; Ma, D.; Ouyang, Z. Lake and Wetland Ecosystem Services Measuring Water Storage and Local Climate Regulation. *Water Resour. Res.* **2017**, *53*, 3197–3223. [CrossRef]
4. Gleeson, T.; Cuthbert, M.; Ferguson, G.; Perrone, D. Global Groundwater Sustainability, Resources, and Systems in the Anthropocene. *Annu. Rev. Earth Planet. Sci.* **2020**, *48*, 431–463. [CrossRef]
5. Marcinkowski, P.; Piniewski, M.; Kardel, I.; Szcześniak, M.; Benestad, R.; Srinivasan, R.; Ignar, S.; Okruszko, T. Effect of Climate Change on Hydrology, Sediment and Nutrient Losses in Two Lowland Catchments in Poland. *Water* **2017**, *9*, 156. [CrossRef]
6. Wang, X.; Liu, Z.; Jun Xu, Y.; Mao, B.; Jia, S. Extreme Drought Affects Lake Water Quality, Quantity, Morphometry: Evidence from China's Largest Fresh Water Lake under the 2022 Global Drought. *Geosci. Front.* **2025**, *16*, 102146. [CrossRef]
7. Wanek, A.; Hargiss, C.L.M.; Norland, J.; Ellingson, N. Assessment of Water Quality in Ponds across the Rural, Peri-Urban, and Urban Gradient. *Environ. Monit. Assess.* **2021**, *193*, 694. [CrossRef]
8. Zhou, J.; Li, Y.; Lei, Q.; Feng, Q.; Luo, J.; Lindsey, S. Asynchrony between Urban Expansion and Water Environmental Protection Reshapes the Spatial Patterns of Nitrogen and Phosphorus Concentrations and N:P Stoichiometry in Inland Small Water Bodies in Changsha, China. *Front. Environ. Sci.* **2022**, *10*, 1018408. [CrossRef]
9. Brehob, M.M.; Pennino, M.J.; Handler, A.M.; Compton, J.E.; Lee, S.S.; Sabo, R.D. Estimates of Lake Nitrogen, Phosphorus, and Chlorophyll-a Concentrations to Characterize Harmful Algal Bloom Risk Across the United States. *Earth's Future* **2024**, *12*, e2024EF004493. [CrossRef]
10. Heisler, J.; Glibert, P.; Burkholder, J.; Anderson, D.; Cochlan, W.; Dennison, W.; Gobler, C.; Dortch, Q.; Heil, C.; Humphries, E.; et al. Eutrophication and Harmful Algal Blooms: A Scientific Consensus. *Harmful Algae* **2008**, *8*, 3–13. [CrossRef]
11. Ansari, A.A.; Gill, S.S.; Lanza, G.R.; Rast, W. (Eds.) *Eutrophication: Causes, Consequences and Control*; Springer: Dordrecht, The Netherlands, 2011; ISBN 978-90-481-9624-1.
12. Kong, X.; Determann, M.; Andersen, T.K.; Barbosa, C.C.; Dadi, T.; Janssen, A.B.G.; Paule-Mercado, M.C.; Pujoni, D.G.F.; Schultze, M.; Rinke, K. Synergistic Effects of Warming and Internal Nutrient Loading Interfere with the Long-Term Stability of Lake Restoration and Induce Sudden Re-Eutrophication. *Environ. Sci. Technol.* **2023**, *57*, 4003–4013. [CrossRef] [PubMed]
13. Li, G.; Zhou, J.; Deng, D.; Du, M.; Meng, Y.; Dai, L.; Peng, Q.; Wang, L. Understanding the Relationship Between Water Quality and Soil Nutrient Dynamics in Qinghai Lake Through Statistical and Regression Models. *Water* **2025**, *17*, 472. [CrossRef]
14. OECD. *Diffuse Pollution, Degraded Waters: Emerging Policy Solutions*; OECD Studies on Water; OECD: Paris, France, 2017; ISBN 978-92-64-26905-7.
15. Devlin, M.; Brodie, J. Nutrients and Eutrophication. In *Marine Pollution—Monitoring, Management and Mitigation*; Reichelt-Brushett, A., Ed.; Springer Nature: Cham, Switzerland, 2023; pp. 75–100, ISBN 978-3-031-10127-4.
16. De Souza Beghelli, F.G.; Frascareli, D.; Pompêo, M.L.M.; Moschini-Carlos, V. Trophic State Evolution over 15 Years in a Tropical Reservoir with Low Nitrogen Concentrations and Cyanobacteria Predominance. *Water. Air. Soil Pollut.* **2016**, *227*, 95. [CrossRef]
17. Raulino, R.N.S.; Andrade de Lima, M.V. Multimodel TSI Evaluation to Characterize Eutrophication in a Tropical Semi-Arid Reservoir: A Case Study of the Araras Reservoir. *Rev. Gest. Ambient. E Sustentabilidade GeAS* **2024**, *13*, 30.

18. Bauer-Gottwein, P.; Gondwe, B.R.N.; Charvet, G.; Marín, L.E.; Rebolledo-Vieyra, M.; Merediz-Alonso, G. Review: The Yucatán Peninsula Karst Aquifer, Mexico. *Hydrogeol. J.* **2011**, *19*, 507–524. [CrossRef]
19. Carrillo, L.; Yescas, M.; Nieto-Oropeza, M.O.; Elías-Gutiérrez, M.; Alcérreca-Huerta, J.C.; Palacios-Hernández, E.; Reyes-Mendoza, O.F. Investigating the Morphometry and Hydrometeorological Variability of a Fragile Tropical Karstic Lake of the Yucatán Peninsula: Bacalar Lagoon. *Hydrology* **2024**, *11*, 68. [CrossRef]
20. Gondwe, B.R.N.; Lerer, S.; Stisen, S.; Marín, L.; Rebolledo-Vieyra, M.; Merediz-Alonso, G.; Bauer-Gottwein, P. Hydrogeology of the South-Eastern Yucatan Peninsula: New Insights from Water Level Measurements, Geochemistry, Geophysics and Remote Sensing. *J. Hydrol.* **2010**, *389*, 1–17. [CrossRef]
21. Lucero, L.J. Ancient Maya Reservoirs, Constructed Wetlands, and Future Water Needs. *Proc. Natl. Acad. Sci. USA* **2023**, *120*, e2306870120. [CrossRef]
22. Instituto Nacional de Estadística y Geografía (INEGI). Available online: https://www.inegi.org.mx/?utm_source (accessed on 24 October 2025).
23. Moreno-Pérez, P.A.; Hernández-Téllez, M.; Bautista-Gálvez, A. In Danger One of the Largest Aquifers in the World, the Great Mayan Aquifer, Based on Monitoring the Cenotes of the Yucatan Peninsula. *Arch. Environ. Contam. Toxicol.* **2021**, *81*, 189–198. [CrossRef]
24. García-Cruz, N.; Couder-García, B.; Saldaña-Villanueva, K.; Valdivia Rivera, S. Capítulo 7 Contaminantes Ambientales En La Península de Yucatán. In *Los Residuos Pesqueros, Zcuícolas y Biomasa de Algas: Posibilidades de su Aprovechamiento en la Península de Yucatán. Experiencias Transdiciplinarias/Sustentables con Enfoque a la Soberanía Alimentaria*; CIATEJ: Guadalajara, Mexico, 2025; pp. 131–149, ISBN 978-607-8734-83-2.
25. Cohuo, S.; Moreno-López, A.; Escamilla-Tut, N.Y.; Pérez-Tapia, A.M.; Santos-Itzá, I.; Macario-González, L.A.; Villegas-Sánchez, C.A.; Medina-Quej, A. Assessment of Water Quality and Heavy Metal Environmental Risk on the Peri-Urban Karst Tropical Lake La Sabana, Yucatán Peninsula. *Water* **2023**, *15*, 390. [CrossRef]
26. Acuña-Alonso, C.; Álvarez, X.; Lorenzo, O.; Cancela, Á.; Valero, E.; Sánchez, Á. Assessment of Water Quality in Eutrophized Water Bodies through the Application of Indexes and Toxicity. *Sci. Total Environ.* **2020**, *728*, 138775. [CrossRef] [PubMed]
27. Kopczynski, S.; Nolen, R.; Hala, D.; Lases-Hernández, F.; Escobedo-Hinojosa, W.; Arcega-Cabrera, F.; Oceguera-Vargas, I.; Quigg, A. Investigation of Anthropogenic and Emerging Contaminants in Sinkholes (Cenotes) of the Great Mayan Aquifer, Yucatán Peninsula. *Arch. Environ. Contam. Toxicol.* **2025**, *89*, 279–299. [CrossRef]
28. Arcega-Cabrera, F.; Sickman, J.O.; Fargher, L.; Herrera-Silveira, J.; Lucero, D.; Oceguera-Vargas, I.; Lamas-Cosío, E.; Robledo-Ardila, P.A. Groundwater Quality in the Yucatan Peninsula: Insights from Stable Isotope and Metals Analysis. *Groundwater* **2021**, *59*, 878–891. [CrossRef] [PubMed]
29. Herrera-Silveira, J.A.; Medina-Gomez, I.; Colli, R. Trophic Status Based on Nutrient Concentration Scales and Primary Producers Community of Tropical Coastal Lagoons Influenced by Groundwater Discharges. *Hydrobiologia* **2002**, *475/476*, 91–98. [CrossRef]
30. Rodríguez-Huerta, E.; Rosas-Casals, M.; Hernández-Terrones, L.M. A Water Balance Model to Estimate Climate Change Impact on Groundwater Recharge in Yucatan Peninsula, Mexico. *Hydrol. Sci. J.* **2020**, *65*, 470–486. [CrossRef]
31. Barats, A.; Renac, C.; Garrido- Hoyos, S.; Gonzalez-Perez, B.; Garcia-Mendoza, K.; Esteller-Alberich, M.V.; Jara-Marini, M.E.; Aguilar-Chavez, A. Assessment of the Water Quality in the Coastal Yaqui Valley (Mexico): Implications for Human Health and Ecological Risks. *Environ. Res.* **2025**, *264*, 120275. [CrossRef]
32. Marisa, M.-H.; Adrián, F.-R.; Jannice, A.-V.; Misael Sebastián, G.-H.; Diego, D.-V. Water Quality Management in a Tropical Karstic System Influenced by Land Use in Chiapas, Mexico. *Environ. Chall.* **2024**, *16*, 100981. [CrossRef]
33. Chidiac, S.; El Najjar, P.; Ouaini, N.; El Rayess, Y.; El Azzi, D. A Comprehensive Review of Water Quality Indices (WQIs): History, Models, Attempts and Perspectives. *Rev. Environ. Sci. Biotechnol.* **2023**, *22*, 349–395. [CrossRef]
34. Perry, E.; Socki, R. Hydrogeology of the Yucatán Peninsula. In *The Lowland Maya Area*; CRC Press: Boca Raton, FL, USA, 2003.
35. Romero, D.; Alfaro, E.J. Spatiotemporal Variability of the Rainy Season in the Yucatan Peninsula. *Int. J. Climatol.* **2024**, *44*, 2561–2574. [CrossRef]
36. Sanchez Rivera, G.; Frausto, O.; Gómez-Mendoza, L.; Terán-Cuevas, Á.; Morales Hernandez, J. Tropical Cyclones in the North Atlantic Basin and Yucatan Peninsula, Mexico: Identification of Extreme Events. *Int. J. Des. Nat. Ecodyn.* **2021**, *16*, 145–160. [CrossRef]
37. Bautista, F. Clasificación de Suelos de La Península de Yucatán. In *Los Territorios Kársticos de la Península de Yucatán: Caracterización, Manejo y Riesgos*; Mexican Association for Karst Studies: Mexico, Mexico, 2021; pp. 25–38, ISBN 978-607-97684-2-3.
38. Strickland, J.D.H.; Parsons, T.R. *A Practical Handbook of Seawater Analysis*; Fisheries Research Board of Canada: Ottawa, ON, Canada, 1972.
39. Jeffrey, S.W.; Humphrey, G.F. New Spectrophotometric Equations for Determining Chlorophylls a, b, C1 and C2 in Higher Plants, Algae and Natural Phytoplankton. *Biochem. Physiol. Pflanz.* **1975**, *167*, 191–194. [CrossRef]
40. Biliani, I.; Skamnia, E.; Economou, P.; Zacharias, I. A Novel Methodology to Correct Chlorophyll-a Concentrations from Satellite Data and Assess Credible Phenological Patterns. *Remote Sens.* **2025**, *17*, 1156. [CrossRef]

41. Metcalf, L.; Eddy, H.P.; Tchobanoglous, G. *Wastewater Engineering: Treatment, Disposal, and Reuse*; McGraw-Hill: New York, NY, USA, 2004; Volume 4.
42. Schumacher, A.J.; Lingle, C.K.; Silbernagel, K.M.; Thompson-Strehlow, L. Validation of the 3M™ Petrifilm™ Coliform Count Plate for Enumeration of Coliforms in Bottled Water: AOAC Performance Tested MethodSM 082101. *J. AOAC Int.* **2021**, *105*, 866–875. [CrossRef] [PubMed]
43. DOTABLES. Available online: https://water.usgs.gov/water-resources/software/DOTABLES/ (accessed on 22 June 2025).
44. Garcia, H.E.; Gordon, L.I. Oxygen Solubility in Seawater: Better Fitting Equations. *Limnol. Oceanogr.* **1992**, *37*, 1307–1312. [CrossRef]
45. WQI. For Surface Waters. Available online: https://form.jotform.com/222877212484056 (accessed on 14 September 2025).
46. Paulic, M.; Hand, J.; Lord, L. *Florida Department of Environmental Protection. 1996 Water-Quality Assessment for the State of Florida, Section 305(b) Main Report*; Florida Department of Environmental Protection: Tallahassee, FL, USA, 1996. Available online: http://lake.wateratlas.usf.edu/upload/documents/1996%20Water-Quality%20Assessment%20for%20the%20State%20of%20Florida%20Section%20305(b)%20Main%20Report.pdf (accessed on 5 September 2025).
47. Kendall, M.G. *Rank Correlation Methods*; Griffin: Oxford, UK, 1948.
48. Mann, H.B. Nonparametric Tests Against Trend. *Econometrica* **1945**, *13*, 245–259. [CrossRef]
49. Theil, H. A Rank-Invariant Method of Linear and Polynomial Regression Analysis. In *Henri Theil's Contributions to Economics and Econometrics*; Raj, B., Koerts, J., Eds.; Advanced Studies in Theoretical and Applied Econometrics; Springer: Dordrecht, The Netherlands, 1992; Volume 23, pp. 345–381, ISBN 978-94-010-5124-8.
50. Souza, T. Non-Metric Multidimensional Scaling (NMDS). In *Advanced Statistical Analysis for Soil Scientists*; Souza, T., Ed.; Springer Nature: Cham, Switzerland, 2025; pp. 79–102, ISBN 978-3-031-88161-9.
51. Hammoumi, D.; Al-Aizari, H.S.; Alaraidh, I.A.; Okla, M.K.; Assal, M.E.; Al-Aizari, A.R.; Moshab, M.S.; Chakiri, S.; Bejjaji, Z. Seasonal Variations and Assessment of Surface Water Quality Using Water Quality Index (WQI) and Principal Component Analysis (PCA): A Case Study. *Sustainability* **2024**, *16*, 5644. [CrossRef]
52. Dutta, S.; Dwivedi, A.; Suresh Kumar, M. Use of Water Quality Index and Multivariate Statistical Techniques for the Assessment of Spatial Variations in Water Quality of a Small River. *Environ. Monit. Assess.* **2018**, *190*, 718. [CrossRef]
53. Zavareh, M.; Maggioni, V.; Sokolov, V.; Zavareh, M.; Maggioni, V.; Sokolov, V. Investigating Water Quality Data Using Principal Component Analysis and Granger Causality. *Water* **2021**, *13*, 343. [CrossRef]
54. McCune, B.; Grace, J.B.; Urban, D.L. *Analysis of Ecological Communities*; MjM Software Design: Gleneden Beach, OR, USA, 2002; ISBN 0-9721290-0-6.
55. Arcega-Cabrera, F.; León-Aguirre, K.; Enseñat-Soberanis, F.; Giácoman-Vallejos, G.; Rodríguez-Fuentes, G.; Oceguera-Vargas, I.; Lamas-Cosío, E.; Simoes, N. Use of Microbiological and Chemical Data to Evaluate the Effects of Tourism on Water Quality in Karstic Cenotes in Yucatan, Mexico. *Bull. Environ. Contam. Toxicol.* **2023**, *111*, 6. [CrossRef]
56. Borbolla-Vazquez, J.; Ugalde-Silva, P.; León-Borges, J.; Díaz-Hernández, J.A. Total and Faecal Coliforms Presence in Cenotes of Cancun; Quintana Roo, Mexico. *BioRisk* **2020**, *15*, 31–43. [CrossRef]
57. Rojas Fabro, A.Y.; Pacheco Ávila, J.G.; Esteller Alberich, M.V.; Cabrera Sansores, S.A.; Camargo-Valero, M.A. Spatial Distribution of Nitrate Health Risk Associated with Groundwater Use as Drinking Water in Merida, Mexico. *Appl. Geogr.* **2015**, *65*, 49–57. [CrossRef]
58. INEGI Mapa. Available online: https://www.inegi.org.mx/app/biblioteca/ficha.html?upc=889463173359&utm (accessed on 18 November 2025).
59. Ellis, E.A.; Romero Montero, J.A.; Hernández Gómez, I.U. Deforestation Processes in the State of Quintana Roo, Mexico: The Role of Land Use and Community Forestry. *Trop. Conserv. Sci.* **2017**, *10*, 1940082917697259. [CrossRef]
60. INEGICenso Agropecuario (CA) 2022. Available online: https://www.inegi.org.mx/programas/ca/2022/ (accessed on 1 September 2025).
61. Tun-Canto, G.E.; Álvarez-Legorreta, T.; Zapata-Buenfil, G.; Sosa-Cordero, E. Metales Pesados En Suelos y Sedimentos de La Zona Cañera Del Sur de Quintana Roo, México. *Rev. Mex. Cienc. Geológicas* **2017**, *34*, 157. [CrossRef]
62. Kauffer Michel, E.F.; Villanueva Aguilar, C.L.V. Retos de la gestión de una cuenca construida: La Península de Yucatán en México. *Aqua-LAC* **2011**, *3*, 81–91. [CrossRef]
63. Camacho-Cruz, K.A.; Ortiz-Hernández, M.C.; Sánchez, A.; Carrillo, L.; De Jesús Navarrete, A. Water Quality in the Eastern Karst Region of the Yucatan Peninsula: Nutrients and Stable Nitrogen Isotopes in Turtle Grass, Thalassia Testudinum. *Environ. Sci. Pollut. Res.* **2020**, *27*, 15967–15983. [CrossRef]
64. Nazeri Tahroudi, M. Comprehensive Global Assessment of Precipitation Trend and Pattern Variability Considering Their Distribution Dynamics. *Sci. Rep.* **2025**, *15*, 22458. [CrossRef]
65. O'Gorman, P.A. Precipitation Extremes Under Climate Change. *Curr. Clim. Change Rep.* **2015**, *1*, 49–59. [CrossRef]

66. Elías-Gutiérrez, M.; Valdez-Moreno, M.; Montes-Ortiz, L.; García-Morales, A.E. Zooplankton as an Indicator: A Dramatic Shift in Its Composition Following a Sudden Temporal Brownification of a Tropical Oligotrophic Lake in Southern Mexico. *Diversity* **2025**, *17*, 58. [CrossRef]
67. Samset, B.H.; Zhou, C.; Fuglestvedt, J.S.; Lund, M.T.; Marotzke, J.; Zelinka, M.D. Steady Global Surface Warming from 1973 to 2022 but Increased Warming Rate after 1990. *Commun. Earth Environ.* **2023**, *4*, 400. [CrossRef]
68. Griffith, A.W.; Gobler, C.J. Harmful Algal Blooms: A Climate Change Co-Stressor in Marine and Freshwater Ecosystems. *Harmful Algae* **2020**, *91*, 101590. [CrossRef]
69. Gogoi, P.; Das, B.K.; Koushlesh, S.K.; Johnson, C.; Malick, R.; Saha, A.; Kayal, T.; Chakraborty, R.; Pradhan, L.; Das, A.K. An Integrative Water Quality Index and Multivariate Modeling Approach to Assess Surface Water Quality, Trophic Status and Nutrient Source Apportionment in a Large Tropical Reservoir, Hirakud–the Longest Earthen Dam in Asia. *Appl. Water Sci.* **2025**, *15*, 219. [CrossRef]
70. INEGI. *XII Censo General de Población y Vivienda 2000*; Instituto Nacional de Estadística y Geografía: Aguascalientes, Mexico, 2001; p. 113. Available online: https://www.inegi.org.mx/programas/ccpv/2000/ (accessed on 5 September 2025).
71. INEGI. *Censo de Población y Vivienda 2020. Resultados Definitivos*; Instituto Nacional de Estadística y Geografía: Aguascalientes, Mexico, 2020. Available online: https://www.inegi.org.mx/programas/ccpv/2020/ (accessed on 5 September 2025).
72. Zhang, Y.; Li, M.; Dong, J.; Yang, H.; Van Zwieten, L.; Lu, H.; Alshameri, A.; Zhan, Z.; Chen, X.; Jiang, X.; et al. A Critical Review of Methods for Analyzing Freshwater Eutrophication. *Water* **2021**, *13*, 225. [CrossRef]
73. Ferguson, A.; Filippini, G.; Potts, J.; Bugnot, A.B.; Johnston, E.L.; Rao, S.; Ruszczyk, J.; Dafforn, K.A. Benthic Processes Are an Important Indicator of Eutrophication in Intermittently Open and Closed Lakes and Lagoons. *Estuaries Coasts* **2024**, *47*, 2324–2340. [CrossRef]
74. Andrietti, G.; Freire, R.; do Amaral, A.G.; de Almeida, F.T.; Bongiovani, M.C.; Schneider, R.M. Water quality index and eutrophication indices of Caiabi River, MT. *Ambiente E Agua-Interdiscip. J. Appl. Sci.* **2016**, *11*, 162–175.
75. Kim, H.-S.; Hwang, S.-J.; Shin, J.-K.; An, K.-G.; Yoon, C.G. Effects of Limiting Nutrients and N:P Ratios on the Phytoplankton Growth in a Shallow Hypertrophic Reservoir. *Hydrobiologia* **2007**, *581*, 255–267. [CrossRef]
76. Heffernan, J.B.; Albertin, A.R.; Fork, M.L.; Katz, B.G.; Cohen, M.J. Denitrification and Inference of Nitrogen Sources in the Karstic Floridan Aquifer. *Biogeosciences* **2012**, *9*, 1671–1690. [CrossRef]
77. Brandenburg, K.; Siebers, L.; Keuskamp, J.; Jephcott, T.G.; Van de Waal, D.B. Effects of Nutrient Limitation on the Synthesis of N-Rich Phytoplankton Toxins: A Meta-Analysis. *Toxins* **2020**, *12*, 221. [CrossRef]
78. Scott, J.; McCarthy, M.; Paerl, H. Nitrogen Transformations Differentially Affect Nutrient-limited Primary Production in Lakes of Varying Trophic State. *Limnol. Oceanogr. Lett.* **2019**, *4*, 96–104. [CrossRef]
79. Trommer, G.; Leynaert, A.; Klein, C.; Naegelen, A.; Beker, B. Phytoplankton Phosphorus Limitation in a North Atlantic Coastal Ecosystem Not Predicted by Nutrient Load. *J. Plankton Res.* **2013**, *35*, 1207–1219. [CrossRef]
80. Yanez-Montalvo, A.; Gómez-Acata, S.; Águila, B.; Hernández-Arana, H.; Falcón, L.I. The Microbiome of Modern Microbialites in Bacalar Lagoon, Mexico. *PLoS ONE* **2020**, *15*, e0230071. [CrossRef]
81. Feng, S.; Zhang, C.; Yan, J.; Ren, K.; Peng, N.; Jiang, W.; Liu, S. Research on the Surface Water Quality in the Huaihe River Basin and the Gensis Based on Multivariate Statistical Analysis. *Sci. Rep.* **2025**, *15*, 19763. [CrossRef]
82. Hu, L.; Chen, L.; Li, Q.; Zou, K.; Li, J.; Ye, H. Water Quality Analysis Using the CCME-WQI Method with Time Series Analysis in a Water Supply Reservoir. *Water Supply* **2022**, *22*, 6281–6295. [CrossRef]
83. Madjar, R.M.; Scăeţeanu, G.V.; Sandu, M.A.; Madjar, R.M.; Scăeţeanu, G.V.; Sandu, M.A. Nutrient Water Pollution from Unsustainable Patterns of Agricultural Systems, Effects and Measures of Integrated Farming. *Water* **2024**, *16*, 3146. [CrossRef]
84. Xu, J.; Mo, Y.; Zhu, S.; Wu, J.; Jin, G.; Wang, Y.-G.; Ji, Q.; Li, L. Assessing and Predicting Water Quality Index with Key Water Parameters by Machine Learning Models in Coastal Cities, China. *Heliyon* **2024**, *10*, e33695. [CrossRef]

Disclaimer/Publisher's Note: The statements, opinions and data contained in all publications are solely those of the individual author(s) and contributor(s) and not of MDPI and/or the editor(s). MDPI and/or the editor(s) disclaim responsibility for any injury to people or property resulting from any ideas, methods, instructions or products referred to in the content.